

Reynolds number dependence of the amplitude modulated near-wall cycle

IVAN MARUSIC, ROMAIN MATHIS AND NICHOLAS HUTCHINS

Abstract The interaction in turbulent boundary layers between very large scale motions centered nominally in the log region (termed superstructures) and the small scale motions is investigated across the boundary layer. This analysis is performed using tools based on Hilbert transforms. The results, across a large Reynolds number range, show that in addition to the large-scale log region structures superimposing a footprint (or mean shift) on to the near-wall fluctuations, the small-scale structures are also subject to a high degree of amplitude modulation due to the large structures. The amplitude modulation effect is seen to become progressively stronger as the Reynolds number increases.

1 Introduction

Advances in numerical simulation, measurement techniques and high Reynolds number facilities have provided the opportunity in recent years to study in greater detail the relationship between eddying motions of different length scales in wall-bounded flows. The near wall-cycle, related to the near-wall streaks described by Kline *et al.* [11], has been largely viewed as depending only on global viscous wall units. The study by Jimenez & Pinelli [7] has shown that this region can self-sustain in the absence of an outer region and it is therefore often referred to as being au-

Ivan Marusic
Department of Mechanical Engineering, University of Melbourne, Victoria 3010, Australia
e-mail: imarusic@unimelb.edu.au

Romain Mathis
Department of Mechanical Engineering, University of Melbourne, Victoria 3010, Australia
e-mail: rmathis@unimelb.edu.au

Nicholas Hutchins
Department of Mechanical Engineering, University of Melbourne, Victoria 3010, Australia
e-mail: nhu@unimelb.edu.au

tonomous. This autonomous view was based largely on an understanding of low Reynolds number flows, which by definition have a limited range of scales of motions. More recently, studies at higher Reynolds number (with high-fidelity measurement or simulation) have shown that the near-wall cycle is affected by the outer flow region ([9, 2, 1, 16, 14, 3, 6]) and hence perhaps should not be considered as purely “autonomous”. Hutchins & Marusic [4] described the large-scale motions responsible for this as “superstructures”, with their origin nominally in the logarithmic region of the boundary layer. These observations came from experiments conducted at a range of Reynolds numbers, and Hutchins & Marusic [4] found that the strength (and influence) of the superstructures increased with increasing Reynolds number. Furthermore, they observed that low-wavenumber energy associated with these very large scale motions is not merely superimposed on the near-wall streamwise fluctuations, but seem to “amplitude modulate” the small-scale fluctuations [5].

This paper is concerned with this amplitude modulation interaction between the large and small (near-wall) scales in turbulent boundary layers. In the remainder of the paper the amplitude modulation effect will be quantified using a correlation coefficient and the effects of increasing Reynolds number will be considered. (A fuller discussion of these effects is given in a paper by Mathis *et al.*[15].)

2 Quantifying amplitude modulation

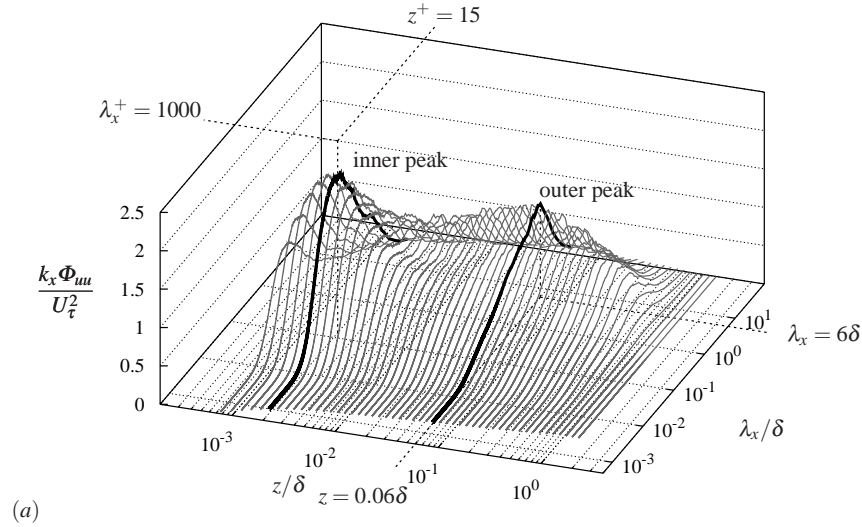


Fig. 1 Pre-multiplied energy spectrogram of streamwise velocity fluctuation $k_x \phi_{uu} / U_\tau^2$ at $Re_\tau = 7300$ across the turbulent boundary layer.

Hutchins & Marusic [4] showed that, at sufficiently high Reynolds numbers, two distinctive peaks appear in the pre-multiplied spectrogram of the fluctuating streamwise velocity, an example of which is shown in figure 1. Here the coordinate system, x , y and z , refers to the streamwise, spanwise and wall-normal directions. The spectral density function of the streamwise velocity fluctuation is described by ϕ_{uu} and the streamwise wavenumber and wavelength are denoted by k_x and λ_x respectively (where $\lambda_x = 2\pi/k_x$). The superscript “+” is used to denote viscous scaling ($z^+ = zU_\tau/\nu$, $u^+ = u/U_\tau$ etc.)

The outer peak is related to superstructures. Hutchins & Marusic [4] showed that a very high level of correlation was found between the filtered (long wavelength) signatures of u simultaneously measured at the locations of the inner and outer peaks. This was understood to mean that the large-structures superimpose their “footprint” near the wall. To quantify the interaction we begin by decomposing the signal from a wall normal location corresponding to the inner peak site ($z^+ = 15$).

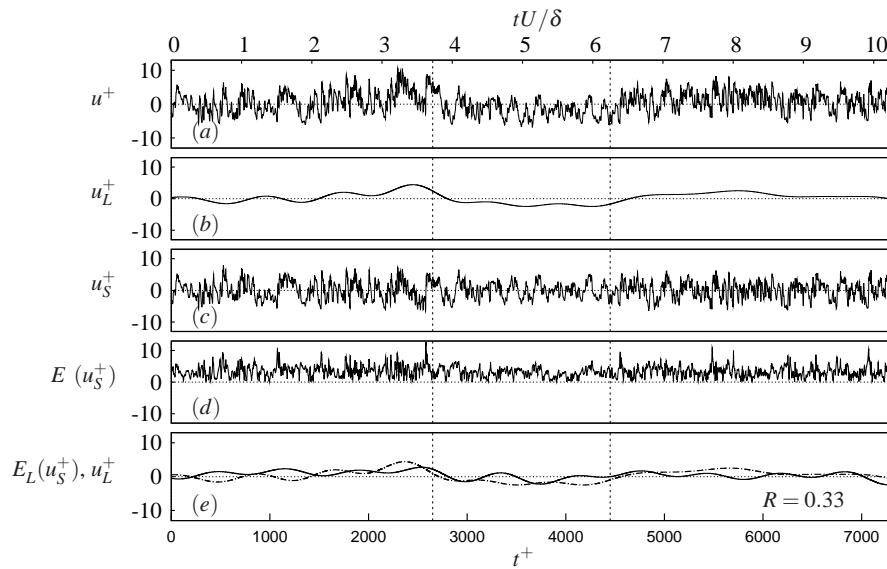


Fig. 2 Example of small-scale decomposition on fluctuating u^+ velocity signal at $z^+ = 15$; (a) the raw signal u^+ ; (b) the large-scale signal u_L^+ ; (c) the small-scale signal u_S^+ ; (d) its envelope; (e) and filtered envelope (solid line) against the large-scale component (dot-dashed). For comparison, the mean of the filtered envelope has been adjusted to zero.

Figure 2 shows a sample of the u signal at $z^+ = 15$ for $Re_\tau = 7300$, as well as its large (u_L) and small (u_S) scale components. Here ‘large’ corresponds to a long-wavelength filtered signal ($\lambda_x > \delta$ retained) and ‘small’ refers to the remainder ($\lambda_x < \delta$). In order to determine the relationship between the large- and small-scale structures contained in any velocity signal, the small-scale component of the signal (u_S^+) is analysed using the Hilbert transformation. This allows us to extract

an envelope ($E(u_S^+)$), representative of any modulating effect (assumed here to be the large-scale component u_L^+). The envelope returned by the Hilbert transformation will track not only the large-scale modulation due to the log region events, but also the small-scale variation in the ‘carrier’ signal. To remove this effect, we filter the envelope at the same cut-off as the large-scale signal ($\lambda_x/\delta > 1$). Hence, a filtered envelope ($E_L(u_S^+)$) describing the modulation of small-scale structures is obtained. It is now possible to compute a meaningful correlation coefficient, R , of the filtered envelope with the large-scale velocity fluctuation u_L^+

$$R = \frac{\overline{u_L^+ E_L(u_S^+)}}{\sqrt{\overline{u_L^{+2}} \overline{E_L(u_S^+)^2}}} \quad (1)$$

where $\sqrt{\overline{u^2}}$ denotes the r.m.s. value of the signal u . For the Reynolds number and signal shown in figure 2, R is found to be 0.33, which is a significant correlation.

3 Experiments

The experiments for this study were conducted in two facilities. The first being the High Reynolds Number Boundary Layer Wind-Tunnel (HRNBLWT) at the University of Melbourne with a working section $27 \times 2 \times 1$ m. Full details of the facility are available in Ref. [17]. Measurements consist of velocity measurements using a single-normal hot-wire probe across the entire boundary layer, and close enough to the wall to measure at the location of the inner peak ($z^+ = 15$). The probe is made using a Wollaston platinum wire sensing element, operated in constant temperature mode using an AA Lab Systems AN-1003 with overheat ratio set to 1.8. For each Reynolds number, the diameter d and length l of the sensing element was adjusted to give a constant viscous scaled length of $l^+ = lU_\tau/\nu = 22$ with $l/d = 200$, to allow comparison without any spatial resolution influences [6]. Measurements were made at five separate Reynolds numbers, namely: $Re_\tau = 2800, 3900, 7300, 13600,$ and 19000 .

The second facility is from very high Reynolds number measurements in the atmospheric surface layer at the SLTEST facility, located at the Great Salt Lake Desert in Western Utah. Full details of the facility are available in references [10], [16] and [12]. The unique geography of this site allows us to obtain measurements in extremely high Reynolds number turbulent boundary layers ($Re_\tau \sim O(10^6)$). The boundary layer develops naturally over 100 km of salt playa, which is remarkably flat and has a low surface roughness. Measurements were performed using an array of 9 logarithmically spaced wall-normal sonic anemometers (Campbell Scientific CSAT3) from $z = 1.4$ to 25.7 m. We will consider here one hour of data taken from a period of prolonged neutral buoyancy and steady wind conditions. Mean statistics were found to compare well with canonical turbulent boundary layers from laboratory facilities [4, 13]. The estimated Reynolds number was $Re_\tau = 650000$.

4 Variations with Reynolds number

Figure 3 presents the pre-multiplied energy spectra maps, $k_x \Phi_{uu}/U_\tau^2$ for all sets of measurements, in the same manner as presented in figure 1, but here simply shown with contour levels. The inner-peak is marked by the “+” symbols and is seen to scale well in viscous units ($z^+ = 15$; $\lambda_x^+ = 1000$) for all cases. The location of the outer peak was found by Hutchins & Marusic [4] to be at $z/\delta = 0.06$ and $\lambda_x/\delta = 6$, but this was based on a study over a limited Reynolds number range. Here, the data in figure 3, which cover a larger Reynolds number range, shows that the location of the outer peak appears to correspond well with the geometric center of the logarithmic region (on a log plot), which is indicated by the vertical dashed lines in the figure. It should be noted that the data from SLTEST are considerably less reliable than the laboratory data, and here are used only as a guide. For the SLTEST data, fluctuating signals (and energy spectra) are only available at 9 locations within the log region.

Figure 4 shows the wall-normal evolution of the degree of amplitude modulation R for all six Reynolds number considered. The global shape of each curve is seen to be the same for all Re_τ . A feature of interest is the wall-normal location at which the degree of amplitude modulation crosses zero. This point delineates the wall-normal position where $R(z^+)$ changes sign, or to be more precise the location at which the amplitude of the small-scale fluctuations is completely *uncorrelated* with the large-scale envelope (i.e. a position with no amplitude modulation), and possibly may be interpreted as the centre of the “source” location of the main modulating motion. The wall-normal position where $R = 0$ (marked with the vertical dashed line) is seen to correspond well with the location of the outer-peak which, as seen in figure 3, agrees well with the nominal mid-point of the log region. Figure 5 shows the location of the zero amplitude modulation for all Reynolds numbers considered here. (It is important to note that the Utah results have large error-bars given the large experimental uncertainties associated with those measurements.) There are considerable differences in the literature as to what constitutes the bounds of the log law. Here, our attention is on a nominal location (rather than a precise one). However, for comparison two lines are shown in figure 5 as estimates of the centre of the logarithmic region (on a log plot). The solid line corresponds to a definition of the log region as $100 < z^+ < 0.15Re_\tau$ giving $z_M^+ = 3.9Re_\tau^{1/2}$, while the dotted line is based on $KRe_\tau^{1/2} < z^+ < 0.15Re_\tau$ giving $z_M^+ = 0.39Re_\tau^{3/4}$, from suggestions by Klewicki *et al.*[8] and others that the lower bound of the log region is Reynolds number dependent.

Overall, the results in figure 3 & 5 support the notion that the outer-peak in the streamwise energy spectra is coincident with the wall-normal location at which the degree of amplitude modulation crosses zero, and that this nominally agrees with the centre of the log region (all of which are Reynolds number dependent). It is difficult to interpret this result within a mechanistic description of the boundary layer. Close to the wall, the positive values of correlation are as expected. A large-scale deviation in the local streamwise velocity, will produce a corresponding change in

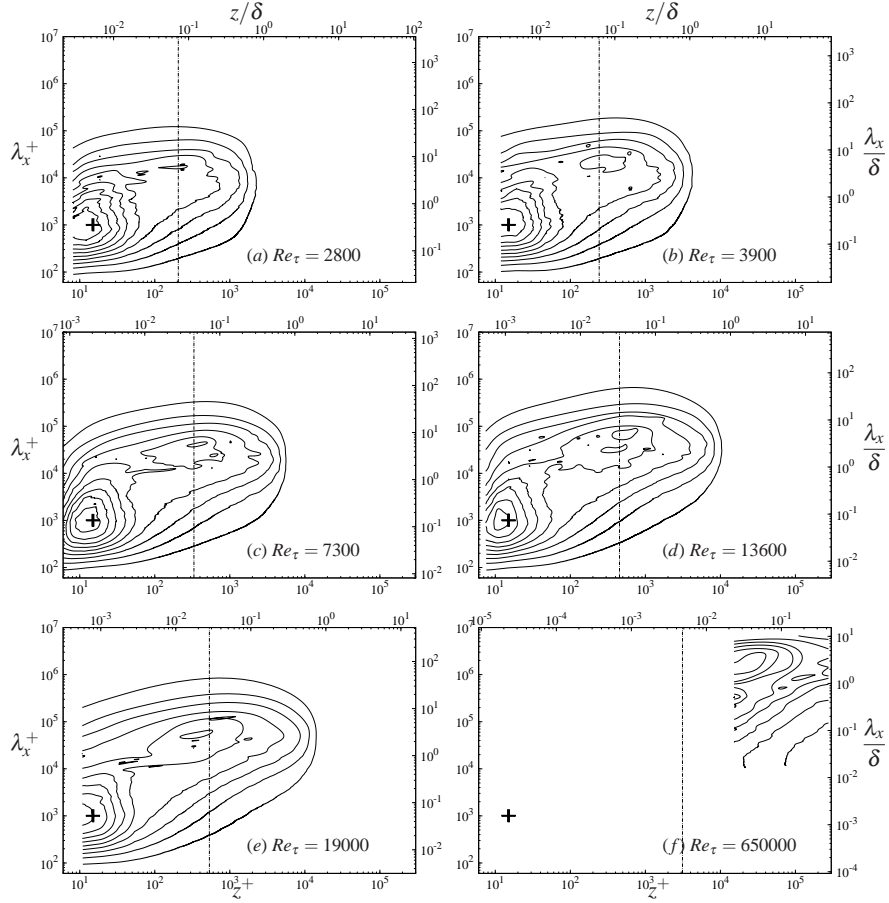


Fig. 3 Reynolds number effect – Iso-contours of the pre-multiplied energy spectra of streamwise velocity fluctuation $k_x \phi_{uu} / U_\tau^2$; (a) $Re_\tau = 2800$; (b) $Re_\tau = 3900$; (c) $Re_\tau = 7300$; (d) $Re_\tau = 13600$; (e) $Re_\tau = 19000$; (f) $Re_\tau = 650000$; Contour levels are form 0.2 to 1.8 in steps of 0.2; The large “+” marks the inner-peak location ($z^+ = 15$, $\lambda_x^+ = 1000$); The vertical dot-dashed line indicates the mid-point of the log-layer.

the local velocity gradient at the wall, altering the turbulence production (or input of vorticity) in the near-wall region. Thus, in this region the magnitude (or envelope) of the small-scale fluctuations would be expected to follow the sign of the large-scale fluctuations (hence positive values of R). Based on the hairpin packet paradigm, one would expect opposite behaviour to occur at some point within the log region. A regime of hairpin packets would imply that most of the small-scale vortical activity would be located within or about the large-scale regions of negative velocity fluctuation (hence the negative values of R in the log region). However, further study is required before a firm conclusion can be made as to why the reversal in sign be-

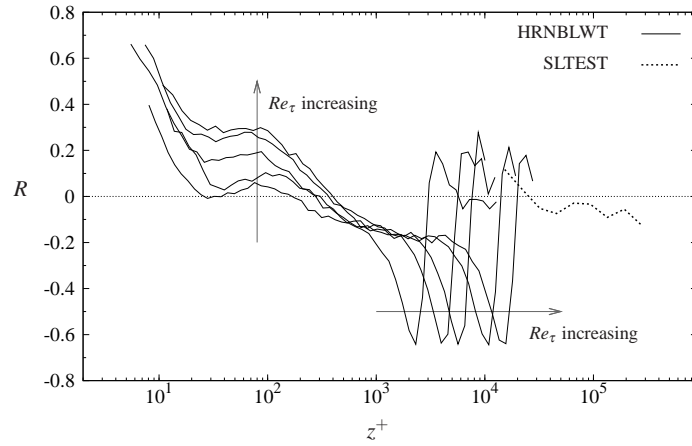


Fig. 4 Wall-normal variation of the degree R of modulation for several Reynolds numbers; $Re_\tau = 2800, 3900, 7350, 13600$ & 19000 from laboratory facility (HRNBLWT); $Re_\tau = 6.4 \times 10^5$ from atmospheric surface layer (SLTEST).

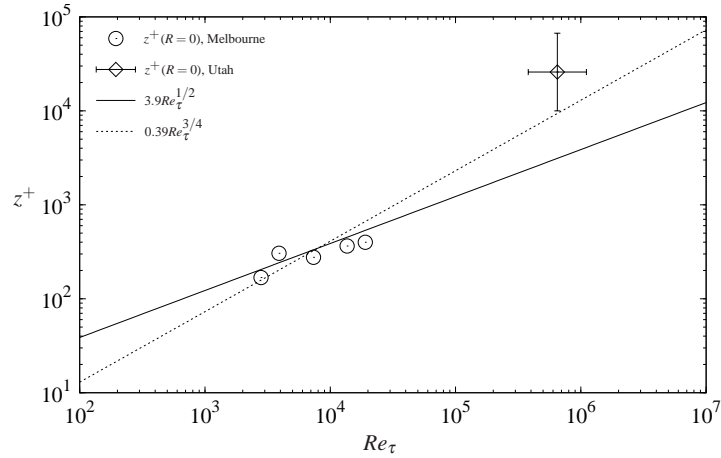


Fig. 5 Wall-normal location where the degree of amplitude modulation reaches zero ($R = 0$) versus Reynolds number. Lines represent estimates for the location of the geometric middle of the log-layer, corresponding to (solid) $100 < z^+ < 0.15Re_\tau$, and (dashed) based on Reynolds number dependant boundaries $KRe_\tau^{1/2} < z^+ < 0.15Re_\tau$ (here $K = 1.2$).

tween these two regions should correspond so well to the location of the ‘outer site’ in the energy spectra.

Acknowledgements We gratefully acknowledge the financial support of the Australian Research Council through grants DP0663499, FF0668703, and DP0984577.

References

1. H. Abe, H. Kawamura, and H. Choi. Very large-scale structures and their effects on the wall shear-stress fluctuations in a turbulent channel flow up to $Re_\tau = 640$. *Trans. ASME: J. Fluid Eng.*, 126:835–843, 2004.
2. D. B. DeGraaff and J. K. Eaton. Reynolds number scaling of the flat-plate turbulent boundary layer. *J. Fluid Mech.*, 422:319–346, 2000.
3. S. Hoyas and J. Jiménez. Scaling of the velocity fluctuations in turbulent channels up to $Re_\tau = 2003$. *Phys. Fluids*, 18:011702, 2006.
4. N. Hutchins and I. Marusic. Evidence of very long meandering features in the logarithmic region of turbulent boundary layers. *J. Fluid Mech.*, 579:1–28, 2007.
5. N. Hutchins and I. Marusic. Large-scale influences in near-wall turbulence. *Phil. Trans. R. Soc. Lond. A*, 365:647–664, 2007.
6. N. Hutchins, T. Nickels, I. Marusic, and M. S. Chong. Spatial resolution issues in hot-wire anemometry. *J. Fluid Mech.*, under review, 2009.
7. J. Jiménez and A. Pinelli. The autonomous cycle of near-wall turbulence. *J. Fluid Mech.*, 389:335–359, 1999.
8. J. Klewicki, P. Fife, T. Wei, and P. McMurty. A physical model of the turbulent boundary layer consonant with mean momentum balance structure. *Phil. Trans. R. Soc. Lond. A*, 365:823–840, 2007.
9. J. C. Klewicki and R. E. Falco. On accurately measuring statistics associated with small-scale structure in turbulent boundary layers using hot-wire probes. *J. Fluid Mech.*, 219:119–142, 1990.
10. J. C. Klewicki, M. M. Metzger, E. Kelner, and E. M. Thurlow. Viscous sublayer flow visualizations at $Re_\theta = 1500000$. *Phys. Fluids*, 7:857–963, 1995.
11. S. J. Kline, W. C. Reynolds, F. A. Schraub, and P. W. Rundstadler. The structure of turbulent boundary layers. *J. Fluid Mech.*, 30:741–773, 1967.
12. G. J. Kunkel and I. Marusic. Study of the near-wall-turbulent region of the high-reynolds-number boundary layer using atmospheric flow. *J. Fluid Mech.*, 548:375–402, 2006.
13. I. Marusic and N. Hutchins. Study of the log-layer structure in wall turbulence over a very large range of Reynolds number. *Flow, Turbulence and Combustion*, 81:115–130, 2008.
14. I. Marusic and G. J. Kunkel. Streamwise turbulence intensity formulation for flat-plate boundary layers. *Phys. Fluids*, 15:2461–2464, 2003.
15. R. Mathis, N. Hutchins, and I. Marusic. Large-scale amplitude modulation of the small-scale structures in turbulent boundary layers. *J. Fluid Mech.*, In Press.
16. M. M. Metzger and J. C. Klewicki. A comparative study of near-wall turbulence in high and low Reynolds number boundary layers. *Phys. Fluids*, 13:692–701, 2001.
17. T. B. Nickels, I. Marusic, S. Hafez, and M. S. Chong. Evidence of the k_1^{-1} law in high-Reynolds number turbulent boundary layer. *Phys. Rev. Lett.*, 95:074501, 2005.